SELECTIVE ADSORPTION OF ANIONIC POLYACRYLAMIDE ONTO ULTRA-LOW ASH COAL AND KAOLINITE

Wenjie ZOU*, Congquan YU*, Chunbao SUN*, Yijun CAO**

* Civil and Environmental Engineering School, University of Science and Technology Beijing, Beijing 100083 China

** National Engineering Research Center of Coal Preparation and Purification, China University of Mining and Technology, Xuzhou 221116 China, wjzou@ustb.edu.cn, zwjcumt@126.com

Abstract: To study the selectivity of polyacrylamide in the selective floc flotation of fine coal, adsorption of anionic polyacrylamide (PAM A401) onto ultra-low ash coal and kaolinite was studied, including the adsorption thermodynamics, floc size distribution and wettability changes. The thermodynamics of the adsorption process at the low concentration of 0-16 mg/dm^3 of PAM A401 were studied at different contact times, doses, temperatures and pH values. Thermodynamic parameters of ΔG^o, ΔH^o, ΔS^o and E_a were evaluated to understand the nature of the adsorption process. The results indicated that PAM A401 was selectively adsorbed onto ultra-low ash coal rather than kaolinite. Physical adsorption was the predominant mechanism, and the adsorption of PAM A401 at 12 mg·dm^{-3} onto coal was 2.15-fold larger than the adsorption on kaolinite. After the adsorption of PAM A401, the lipophilic hydrophilic ratio (LHR) of coal decreased from 9.23 to 7.28, indicating that the coal became less hydrophobic than before. In contrast, the LHR of kaolinite increased from 1.44 to 1.65. Floc size measurements showed that the d_{10}, d_{50} and d_{90} of coal flocculated by PAM A401 (at 12 mg/dm^3, pH 6.5) were 3.18, 2.76 and 2.59-fold greater than the corresponding levels of these parameters for kaolinite flocs, respectively.

Keywords: *coal, kaolinite, anionic polyacrylamide, adsorption, flotation*

Introduction

Flocculation using polyacrylamide involves the mineral processing. For the selective flocculation flotation of fine coal, selective adsorption of flocculants onto the surface of coal or impure minerals is crucial. The surface heterogeneity of coal and clay mineral particles is needed to understand the interaction of clay and coal particles having adsorbed polyacrylamide. Coal is considered to be a heterogeneous mixture and to consist largely of an organic macromolecular matrix with varying degrees of crosslinking where smaller molecular phases are embedded or adsorbed to the

macromolecular network (Mao et al., 2010). On average, clays account for 60–80% of the total impure minerals in coal (Xu et al., 2003). Kaolinite, as the most common clay, is a variety of 1:1 layer silicate having the general formula $Al_2O_3 \cdot 2SiO_2 \cdot 2H_2O$ with two different basal cleavage faces. One basal face consists of tetrahedral siloxane (–Si–O–Si–) species, while the other face consists of an octahedral alumina (Al_2O_3) sheet (Van Olphen and Hsu, 1978). The adsorption of polyacrylamide on to kaolinite was attributed to the hydrogen bonding between the silanol and alumino-OH groups at the particle surface and polymer's primary amide functional groups. Electrostatic attractions or repulsion between the charged polyacrylamide and the negatively charged kaolinite surface was also effect on the adsorption (Nasser and James, 2006; Sabah and Erkan, 2006). Polymeric flocculants were reported to adsorb strongly onto coal (Hogg, 1980). Spencer and Brookes (1987) attributed the flocculation selectivity (when working with mixtures of coal and shale) to the preferential adsorption of flocculant onto coal over shale. The multivalent ions were indicated to act as a bridge between negatively charged coal and kaolinite with anionic groups of the polyacrylamide (Sabah and Erkan, 2006). The selective adsorption of polymers involving dextrin, guar and amylose polysaccharide onto hydrophobic solids such as talc and coal is possibly associated with hydrophobic bonding (Miller et al., 1983; Jenkins and Ralston, 1998; Parolis et al., 2005; Sedeva et al., 2010).

The selective interaction of polyacrylamide with coal and kaolinite and the associated changes in the surface properties were generally not well understood. The beneficial or detrimental effect of floc size enlargement and surface modification on selective flocculation flotation was less reported in related research. Thus, in this study, an attempt was made to clarify the adsorption behavior of anionic polyacrylamide on kaolinite and coal using adsorption thermodynamics, wetting process measurements, floc size measurements and flotation tests. This research is of great significance for the performance judgment and selection of polyacrylamide in selective flocculation of fine coal.

Experimental

Materials

The anionic polyacrylamide (PAM A401, chemically pure) was provided by Xitao Polymer Co., Ltd. Beijing, China. The detailed characteristics and the chemical formula of PAM A401 were given in Table 1. Prior to flocculation tests, a homogeneous stock solution (0.1% w/v) of PAM A401 was prepared using deionized water. This stock solution was diluted to 100 mg·dm^{-3} for flocculation. The deionized water used in the experiments was distilled before further purification through ion-exchange resins (Milli-Q).

Table 1. Characteristics of the anionic polyacrylamide

Name	Ionic Type	Molecular Weight ($\cdot 10^6$ g·mol^{-1})	Charge Density (%)	Chemical formula
A 401	Anionic	3	20	$\left[\begin{smallmatrix}H_2\\C\text{-}CH\end{smallmatrix}(CONH_2)\right]_X\left[\begin{smallmatrix}H_2\\C\text{-}CH\end{smallmatrix}(CO(ONa))\right]_y$

Highly pure kaolinite was obtained from Yongcheng in the Henan Province of China. Figure 1 showed the X-ray diffraction (XRD) patterns of kaolinite. Kaolinite samples contained a small amount of quartz. The chemical analysis of the kaolinite performed by the X-ray fluorescence (XRF) method was presented in Table 2. The total content of Al_2O_3 and SiO_2 of kaolinite was 92.37%. This kaolinite sample contains 54.06% particles below 20 μm measured by a Microtrac S3500 laser diffractometer. The d_{50} and average spherical diameter of the kaolinite sample were 17.5 μm and 21.34 μm, respectively. The sample has a BET nitrogen surface area of 2.81 m^2·g^{-1} determined using a BELSORP-max, Japan and exhibits a point of zero charge (pzc) at pH 2.2 as seen in Fig. 2.

The ultra-low ash coal (ash content 2.60%) was separated by a heavy liquid (1.3 g·cm^{-3}) from clean coal obtained the from the Qianjiaying coking coal preparation plant in the Hebei Province of China. It was dry-ground by a porcelain ball mill of the laboratory type (QHJM-2) for 10 min at 200 rpm, 45% filling rate. The ground ultra-low ash coal contains 60.45% particles below 20 μm, and the d_{50} and average spherical diameter were 13.76 μm and 16.20 μm, respectively. The BET surface area was 2.95 m^2·g^{-1}. This coal sample was a type of bituminous coal with a low oxygen content as seen from the elemental analysis of the ultra-low ash coal in Table 3. This ultra-low ash coal sample was used in adsorption studies, wetting process measurements and floc size measurements.
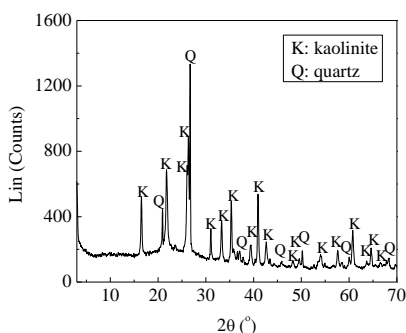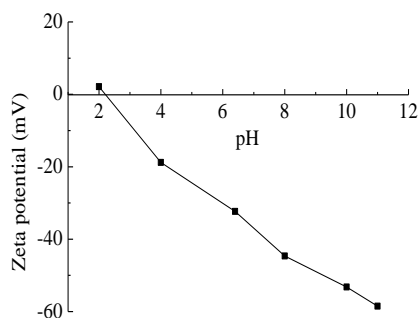

Fig. 1. X-ray diffraction pattern of kaolinite

Fig. 2. Zeta potential of kaolinite pH-zeta of kaolinite suspension in 1 mM KCl as a function of pH measured using the ZetaPALS

Table 2. Chemical composition of kaolinite by XRF

Chemical composition	Al_2O_3	SiO_2	Fe_2O_3	CaO	MgO	Na_2O	K_2O	Ti_2O	P_2O_5
Content (%)	45.84	46.53	0.31	0.16	0.068	0.23	1.09	0.86	0.16

Table 3. Elemental analysis of the ultra-low ash coal sample

Chemical element	C_{daf}	H_{daf}	N_{daf}	$Sulfur_{t, daf}$	O_{daf}
Content (%)	85.72	5.79	1.81	1.35	5.33

daf: dry ash – free basis; t: total

The other coal sample (ash content 32.1%) was the middling of the two-stage flotation process from the Qianjiaying coking coal preparation plant. The coal sample was dry-ground for a certain time. After being ground, the coal sample contained 87.3% particles below 45 μm. This fine coal sample was used in the selective flocculation flotation test.

Methods

Adsorption studies

Adsorption of PAM A401 onto coal or kaolinite surface was estimated by determining the depletion of PAM A401 from the solution using a batch equilibrium procedure. Adsorption experiments were carried out in 250 cm^3 flasks by mixing 1.0000 g coal or kaolinite with 100 cm^3 PAM A401 solution. The suspension was agitated by a rotating shaker at a speed of 200 rpm. The equilibrium time was measured for contact durations ranging from 10 to 180 min and at 20 °C. The pH was adjusted in the range of 2 to 11 by the addition of analytical grade HCl and NaOH, and measured by the same pH electrode. The thermodynamic parameters of the adsorption were established by conducting the experiments at 20, 25, 30, 35 and 40 °C in a temperature-controlled mechanical shaker. The supernatants were then separated from the sediment by centrifugation. Equilibrium concentrations of PAM A401 were determined with a Unico UV/VIS double beam spectrophotometer using a 1 cm quartz cell. Color complexation of the supernatant involved using a starch-CdI$_2$ solution, and the blue solution formed was quantified at 574 nm against a series of standards as outlined by Scoggins and Miller (1979). The experimental error in the colorimetric techniques was ±5 ppm with respect to polyacrylamide concentration (detection range of 0.1–60 mg·dm^{-3}). All the adsorption experiments were duplicated to ensure accuracy and the average errors were about ±2%.

The mean polyacrylamide adsorbed by coal or kaolinite was determined using a mass balance equation expressed as:

$$q_e = \frac{(C_o - C_e) \times V}{m} \tag{1}$$

where q_e is polyacrylamide adsorption per unit weight at equilibrium (mg·g^{-1}), C_o is the initial polyacrylamide concentration in the solution (mg·dm^{-3}), C_e is the polyacrylamide concentration in the solution at equilibrium (mg·dm^{-3}), V is the volume of the initial polyacrylamide solution used (dm^3), and m is the mass of coal or kaolinite used (g).

The Langmuir equation was chosen for the estimation of maximum adsorption capacity corresponding to the coal or kaolinite surface saturation. The linearized form of the Langmuir model after rearrangement is given below:

$$\frac{C_e}{q_e} = \frac{C_e}{q_m} + \frac{1}{K_L q_m} \tag{2}$$

where C_e is the polyacrylamide concentration in solution at equilibrium (mg·dm^{-3}), q_m is the maximum adsorption upon complete saturation of the coal or kaolinite surface (mg·g^{-1}), q_e is polyacrylamide adsorption per unit weight at equilibrium (mg·g^{-1}), and K_L is a constant related to the adsorption/desorption energy. The experimental data were fitted into Eq. (2) for linearization by plotting C_e/q_e against C_e.

The Freundlich model was chosen to estimate the adsorption intensity of the sorbent towards the coal or kaolinite and the linear form is represented by Eq. (3):

$$\ln q_e = \frac{1}{n} \ln C_e + \ln K_F \tag{3}$$

where q_e is polyacrylamide adsorption per unit weight at equilibrium (mg·g^{-1}), C_e is the polyacrylamide concentration in solution at equilibrium (mg·dm^{-3}), and K_L and n are the Freundlich constants. The value of n indicates the affinity of the sorbent towards coal or kaolinite. The experimental data were fitted into Eq. (3) for linearization by plotting $\ln q_e$ against $\ln C_e$. The constants $1/n$ and $\ln K_F$ can be determined from the slope and intercept, respectively.

Thermodynamic parameters associated with the adsorption are standard free energy change (ΔG^o), standard enthalpy change (ΔH^o), standard entropy change (ΔS^o) and activation energy (E_a) and were calculated as follows.

The free energy of the adsorption process, considering the adsorption distribution coefficient K_o, is given by Eq. (4):

$$\Delta G^\Theta = -RT \ln K_o \tag{4}$$

where ΔG^o is the standard free energy of change (kJ·mol^{-1}), R is the universal gas constant (8.314 J·mol^{-1}·K^{-1}), T is the temperature in Kelvin, and K_o is the thermodynamic equilibrium constant. The values of K_o for the adsorption process were determined by plotting $\ln(q_e/C_e)$ against q_e at different temperatures and extrapolating to zero q_e according to the method of Khan and Singh (1987).

Enthalpy change (ΔH^o) and entropy change (ΔS^o) may be determined using the relationships as a function of temperature:

$$\ln K_o = \frac{\Delta H^\Theta}{RT} + \frac{\Delta S^\Theta}{R} \tag{5}$$

where ΔH^o is the standard entropy change (kJ·mol^{-1}), and ΔS^o is the standard entropy change (kJ·mol^{-1}). The values of ΔH^o and ΔS^o can be obtained from the slope and intercept of a plot of $\ln K_o$ against $1/T$.

The sticking probability $S*$ can be expressed as:

$$S^* = (1-\theta)\exp-(\frac{E_a}{RT}) \tag{6}$$

where θ is the surface coverage,

$$\theta = \left(1 - \frac{C_e}{C_o}\right) \tag{7}$$

where C_o and C_e are the initial and equilibrium polyacrylamide concentrations, respectively. The plot of $\ln(1-\theta)$ against $1/T$ will give a linear plot with an intercept of $\ln S*$ and slope of E_a/R.

Wetting process measurement

A Kruss Tensiometer K100 was used for this measurement according to method mentioned in the literature (Zou et al., 2013). The *n*-hexane and water were chosen as the probe liquid in the wettability experiments (Chang et al., 2009). The components of surface free energy of *n*-hexane have disperse part only, the surface tension was 18.4 mN·m^{-1} at 20 °C, and the viscosity of *n*-hexane was low. In each case, the average of five measurements was used.

According to the literatures (Washburn, 1921), there is:

$$\omega^2 = r_{eff}\varepsilon^2(\pi R^2)^2 \frac{\rho^2\gamma\cos\theta}{2\eta}t. \tag{8}$$

If $c = r_{eff}\varepsilon^2(\pi R^2)^2$, then:

$$\omega^2 = c\frac{\rho^2\gamma\cos\theta}{2\eta}t. \tag{9}$$

The slope of the ω^2-t line was k, so there is:

$$k = c\frac{\rho^2 \gamma \cos\theta}{2\eta} \qquad (10)$$

where ω is the liquid weight gain (g), and r_{eff} is the effective radius of the capillary (μm), ε is the porosity, R is the radius of the packed bed (mm), ρ is the density of the liquid (g·cm^{-3}), γ is the surface tension of the liquid (mN·m^{-1}), η is the liquid viscosity (mN·m^{-2}·s^{-1}), θ is the contact angle ($^{\circ}$), and t is the wetting time (s), c is the geometric factor of the packed bed (cm^5).

When k_A and k_B are the slopes of the ω^2-t lines of the oil and water phase separately, the LHR is calculated as follows (Zou et al., 2013):

$$\text{LHR} = \frac{\cos\theta_A}{\cos\theta_B} = \frac{k_A \eta_A}{k_B \eta_B} \cdot \frac{\rho_B^2 \gamma_B}{\rho_A^2 \gamma_A} . \qquad (11)$$

Floc size measurement

The suspension of coal or kaolinite was prepared in deionized water. The concentration of solid suspension was determined by gravimetrically (10 g·dm^{-3}). The suspension was dispersed by ultrasonication for 3 minutes. The deionized water or PAM A401 solution (100 cm^3) was added into the sample cell of a Microtrac S3500 laser diffractometer (measurement range: 0.02–2800 μm), and then the suspension of coal or kaolinite was added dropwise until the detection limit of the instrument was reached. Dynamic floc size was measured during the flocs growth and the sample was circulated through transparent plastic tubing of 5 mm inner diameter by means of a peristaltic pump at a flow rate of 25 cm^3·min^{-1} and then flowed back to the sample cell. The maximum measured value was taken as the floc size distribution under the same mixing intensity (Taylor et al., 2002).

Selective floc flotation test

A flotation cell (XFDM) was used for coal flotation tests with 150 g coal after grinding. Sodium hexametaphosphate in 1.5 dm^3 water at a dosage of 1500 g per Mg was first added, and then the suspension was conditioned at 1800 rpm for 2 min at room temperature. Then, the flocculant of PAM A401 was added. The suspension continued conditioning at 1000 rpm for 5 min, and n-dodecane (700 g/Mg) and 2-octyl alcohol at a dosage of 200 g·Mg^{-1} were added in sequence. Air flow rate was 0.2 m^3·h^{-1}. The froth concentrates and flotation tailings were filtered, dried (in an oven at 105 °C), weighed and taken for ash determination. The errors of weight of products and feed were less than ±2%, the errors of weighted average ash content of products and feed were less than ±1%. The ash of coal sample was determined according to the China national standard of proximate analysis of coal- Instrumental method (GB/T 30732-2014).

Results and discussion

Adsorption equilibrium

The adsorption of PAM A401 was investigated as a function of contact time in the range of 10 to 180 min with 12 mg·dm^{-3} as the initial PAM A401 concentration at 20 °C, as shown in Fig. 3. During the initial 40 min, the higher PAM A401 concentration led to the faster adsorption rate, and the adsorption of PAM A401 onto coal grew faster than that of kaolinite. Following the adsorption process, the adsorption rate of PAM A401 gradually slowed because of fewer adsorption active sites on the surface of the particles and lower PAM A401 concentration. Saturation was nearly reached after 180 min. Hence, 180 min was fixed as the period of contact for further studies. Then experiments were carried out with various dosages ranging from 4 to 16 mg·dm^{-3} as the initial PAM A401 concentration. Figure 4 showed a sharp initial rise in adsorption with the increase of the dose and then an adsorption plateau was attained. The growth of equilibrium adsorption at 12 mg·dm^{-3} slowed down, approaching the saturated adsorption quantity of coal and kaolinite. Thus, the dosage was fixed at 12 mg·dm^{-3} for further studies. The coal adsorbed amount of PAM A401 was 2.15 times larger than that of the kaolinite.

Figure 5 presented the adsorption characteristics of PAM A401 onto coal or kaolinite at acidic, near neutral, and alkaline pH. The adsorption density of PAM A401 onto coal or kaolinite was highly dependent on pH. The adsorbed amount of PAM A401 onto kaolinite at pH 2 was 7.5 times of the adsorbed amount at pH 11. In addition, the adsorption of PAM A401 onto coal was still higher than the adsorption onto kaolinite.

In an environment of high H$^+$ concentration, the native chain conformation of PAM A401 was supposed to be in a state of highly coiled form covering less area on the surface of particles. Moreover, the point of zero charge of kaolinite (pH$_{pzc}$= 2.2) was very close to pH 2. The surface of kaolinite was almost neutral at pH 2 and resulted in lower double layer repulsion thereby increasing the adsorption of the PAM A401 on the surface of kaolinite. At pH 6.4, the surface charge of kaolinite became negative and resulted in higher double layer repulsion thereby reducing the adsorption of the PAM A401 at the surface.

At the alkaline pH of 11, due to the presence of high OH$^-$ ions in the liquid phase, the molecule of PAM A401 was expected to have a highly expanded conformation covering more area on the surface of particles (Caulfield et al., 2002). Moreover, the kaolinite surface at this pH condition was highly negatively charged. The net effect of the above factors resulted in very low adsorption density of the PAM A401 on kaolinite, and consequently leads to negligible flocculation. Because of the -OH groups on the coal surface, the coal surface was almost neutral at pH 2 and negatively charged at near neutral pH and alkaline pH. The trends of adsorption characteristics of PAM A401 onto coal or kaolinite at acidic, near neutral, and alkaline pH were consisted with that of kaolinite. The adsorption of PAM A401 onto coal was higher

than the adsorption onto kaolinite. The hydrophobic interaction was supposed to exist between the surface of coal and hydrocarbon chain of PAM A401. On the basis of the conformational state of the polymer, it could be assumed that the adsorbed layer thickness was expected to increase in the following order of pH: $2 < 4 < 6.5 < 8 < 11$.
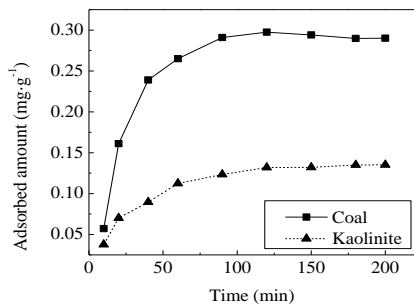

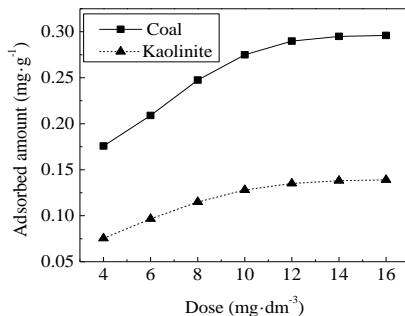Fig. 3. Effect of contact time on the PAM A401 adsorption onto coal and kaolinite

Fig. 4. Effect of initial PAM A401 concentration on the equilibrium adsorption at pH 6.5
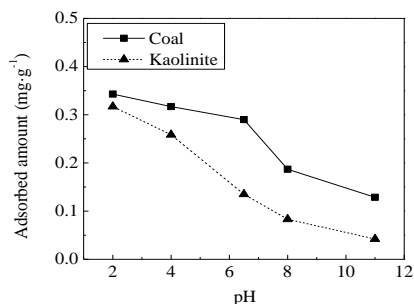

Fig. 5. Effect of pH on the PAM A401 adsorption onto coal and kaolinite
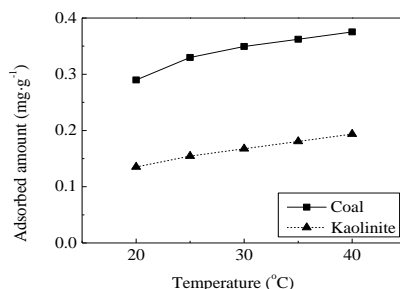
Fig. 6. Effect of temperature on the PAM A401 adsorption onto coal and kaolinite

As seen in Figure 6, temperature clearly influenced the adsorption of PAM A401 onto the coal or kaolinite surface: the adsorption of PAM A401 increased with temperature. However, the adsorption of PAM A401 onto kaolinite was still lower than the absorbance onto coal. The adsorption of PAM A401 increased from 0.29 mg·g^{-1} at 20 °C to 0.375 mg·g^{-1} at 40 °C.

Two classical isotherm models were used to fit the experimental data: the Langmuir and Freundlich models (Besra et al., 2004; Paria and Khilar, 2004). The adsorption isotherm parameters for PAM A401 adsorbed onto coal or kaolinite were shown in Table 4. The isotherm values fit well for both Langmuir and Freundlich isotherms. The Langmuir model (correlation coefficient, i.e., R^2 of 0.9981) fit better than the Freundlich model (R^2 of 0.9854) for coal as well as for kaolinite when compared with the two adsorption models. The better fit to the Langmuir isotherm

model for both coal and kaolinite indicated that the monolayer adsorption was dominant. The K_L of coal (0.3569) was higher than the K_L of kaolinite (0.1945), which indicated that coal held a larger adsorption capacity than kaolinite. The maximum PAM A401 adsorption capacity of coal was 0.3764 mg·g^{-1}, which was higher than the adsorption capacity of kaolinite (0.1982 mg·g^{-1}).

The thermodynamic parameters of ΔG^o, ΔH^o, ΔS^o, E_a and $S\ast$ were calculated from Eqs. (4), (5), (6) and (7) and were presented in Table 5.

Table 4. Adsorption isotherm parameters for PAM A401 adsorbed onto coal or kaolinite

Isotherms			Langmuir Model		Freundlich Model	
Parameters	Coal	Kaolinite	Parameters	Coal	Kaolinite	
q_m	0.3764	0.1982	K_F	0.1325	0.0454	
K_L	0.3569	0.1945	n	2.8385	2.1739	
R^2	0.9981	0.9869	R^2	0.9854	0.9717	
Linear form	$C_e/q_e = 2.6569C_e + 7.4434$	$C_e/q_e = 5.0445C_e + 25.936$	Linear form	$\ln q_e = 0.3523 \ln C_e - 2.021$	$\ln q_e = 0.46 \ln C_e - 3.0912$	

Table 5. Thermodynamic parameters for the PAM A401 adsorption process

Thermodynamic Constant	Temperature	Coal	Kaolinite
K_o	293.15	293.56	54.54
	303.15	820.41	106.79
	313.15	1645.50	160.63
ΔG^o (kJ·mol^{-1})	293.15	-13.849	-9.746
	303.15	-16.911	-11.772
	313.15	-19.281	-13.224
ΔH^o (kJ·mol^{-1})		65.893	41.317
ΔS^o (J·mol^{-1}·K^{-1})		272.392	174.494
E_a (kJ·mol^{-1})		3.780	2.155
$S\ast$		0.160	0.366

The negative values of ΔG^o indicate the spontaneous nature of the adsorption of PAM A401 onto coal or kaolinite. The value of ΔG^o up to -20 kJ·mol^{-1} was consistent with electrostatic interaction between the adsorption sites and PAM A401 (physical adsorption) (Jenkins and Ralston, 1998). The ΔG^o values of coal and kaolinite were -13.839 kJ·mol^{-1} and -9.746 kJ·mol^{-1}, respectively, at 293.15 K, indicating that physical adsorption was the predominant mechanism in the adsorption process. Smaller ΔG^o were associated with stronger adsorption reaction driving forces. Thus, coal had a stronger adsorption reaction driving force for the PAM A401 than kaolinite. The positive values of ΔH^o and E_a for PAM A401 onto coal or kaolinite confirmed the endothermic nature of the adsorption process (Zhu et al., 2010), supported by the

increasing adsorption of PAM A401 with the temperature. Larger positive values of ΔS^o were associated with more random adsorption processes. Thus, the adsorption of PAM A401 onto coal showed a high degree of randomness. A high degree of freedom for the adsorption process confirmed the physical adsorption as well as the relatively low values of ΔG^o. The sticking probability, S^*, was dependent on the property of adsorbate/adsorbent and temperature. The S^* values of coal and kaolinite were found to be $(0 < S^* < 1)$, which indicated that the adsorption followed a physisorption mechanism (Horsfall and Spiff, 2005).

From studies of dextrin adsorption onto hydrophobic coal, Miller et al. (1983) calculated values for ΔG^o ranging between -2.5 and -3.3 kJ·mol^{-1} for the transfer of one -CH$_2$- group from the bulk aqueous solution to the coal surface. From the literature (Pearse, 2005), the hydrophobic effect was due to the attraction of hydrophobic moieties, which may form part of a polymer chain to ''escape'' the aqueous environment and attach to less polar surroundings. We speculated that the hydrophobic effect plays an important role between PAM A401 and the hydrophobic coal surface.

Floc size

Different adsorptions of PAM A401 led to different amounts of flocculation between coal and kaolinite. The difference can be shown through the floc size distribution. In this study, the deionized water was used, and the amount of coal or kaolinite and the PAM A401 dosage were kept constant. Therefore, only the particle types and pH were expected to influence the floc size distribution. Fig. 7 showed that the size distribution peaks of coal and coal with adsorbed PAM A401 were relatively independent at pH 6.5. The size distribution peaks of kaolinite and kaolinite with adsorbed PAM A401 were more overlapping. Thus, the flocculation effect of PAM A401 on kaolinite was significantly lower than the flocculation effect of PAM A401 on the coal. The flocculation selectivity of PAM A401 onto coal was better. This result was consistent with those of the adsorption studies.
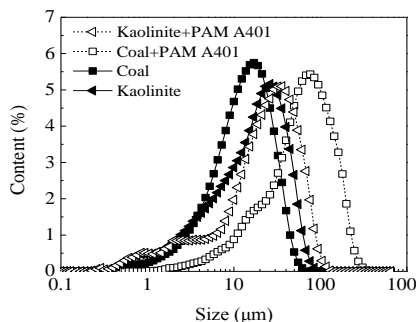

Fig. 7. Effect of PAM A401 on
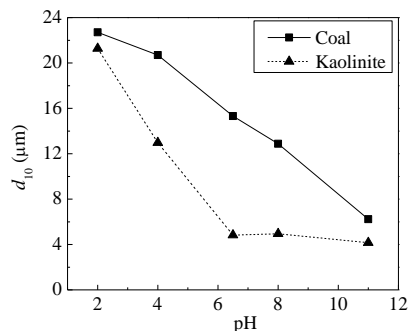the size distribution

Fig. 8. Effect of pH on d_{10} of coal and kaolinite
of coal or kaolinite floc (pH 6.5)

The relevant particle size indicators were d_{10}, d_{50} and d_{90}, which represented the maximum diameters of 10%, 50% and 90%, respectively, of the cumulative volume distributions of the particles (i.e., 10% of the cumulative volume distribution of the particles had a diameter smaller than d_{10}, 50% smaller than d_{50} and 90% smaller than d_{90}). The smaller the d_{10}, the finer the particles were. The larger the d_{90}, the larger the particles were. The d_{50} can be characterized as the average size of the particle sample (Zhang et al., 2012; Taylor et al., 2002). The effects of the pH on d_{10}, d_{50} and d_{90} of coal and kaolinite (12 mg·dm^{-3}) were shown in Figs. 8, 9 and 10, respectively.

At pH 6.5, the coal adsorption of PAM A401 was 2.15 times larger than the coal adsorption of PAM A401 on kaolinite. Meanwhile, the values of d_{10}, d_{50} and d_{90} for coal floc were 3.18, 2.76 and 2.59 times those of kaolinite floc, respectively. Under acidic conditions, the floc size increased significantly with the decrease in pH. The rate of increase of the kaolinite floc was faster than the rate of increase of the coal floc. When pH >7, the floc size of both coal and kaolinite decreased with the increase in pH. The floc size was still larger than coal or kaolinite without PAM A401. The size difference between coal and kaolinite was the largest at pH 6.5. The floc size distribution coincided well with the adsorption test. When the mineral particle size increased to the appropriate range, the collision probabilities of particles and bubbles increased.
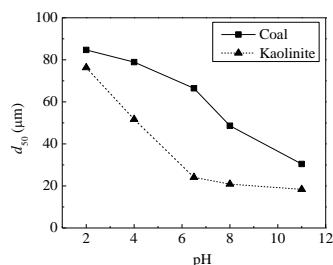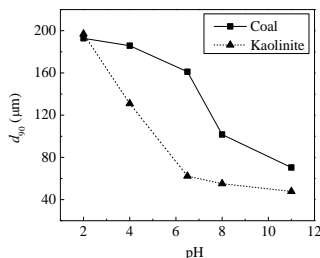

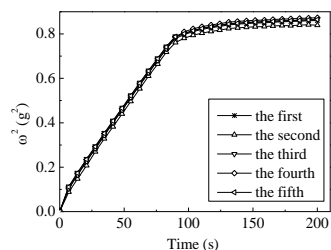Fig. 9. Effect of pH on d_{50} Fig. 10. Effect of pH on d_{90} Fig. 11. The reproducibility tests for coal wetted by *n*-hexane

Wettability changes

The different adsorptions of PAM A401 led to different floc size distributions. The selective enlargement of the coal particle size benefited the fine coal flotation. However, the adsorption of PAM 401 also changed the wettability of coal and kaolinite. The physical parameters of the probe liquids were shown in Table 6. The physicochemical parameters of $\gamma^{LW}_{,s}$ was the non-polar part of the surface tension (mN·m^{-1}), $\gamma^{+}_{,s}$ the acid part of the polar part (mN·m^{-1}) and $\gamma^{-}_{,s}$ the base part of the polar part (mN·m^{-1}). Five experimental curves of the ultra-low ash coal wetting by *n*-hexane were shown in Fig. 11. The average slope and mean variation were 8.23·10^{-3} ±2.7·10^{-5}.

Table 6. Physical parameters of the probe liquids (at 20 °C)

Probe Liquids	Density (g·cm^{-3})	Viscosity (mPa·s)	Surface Tension (mN·m^{-1})	$\gamma^{LW}_{,s}$ (mN·m^{-1})	$\gamma^{+}_{,s}$ (mN·m^{-1})	$\gamma^{-}_{,s}$ (mN·m^{-1})
n-Hexane	0.661	0.326	18.4	18.4	0	0
Deionized water	0.998	1.002	72.8	21.8	25.5	25.5
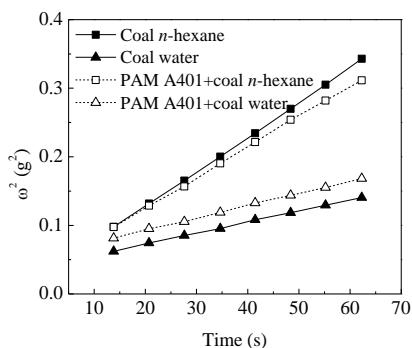
Fig. 12. Wetting curves by *n*-hexane and water of coal
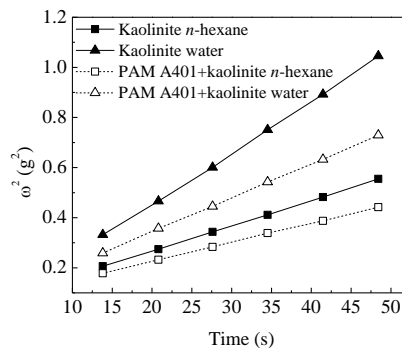
Fig. 13. Wetting curves by *n*-hexane and water of kaolinite

Table 7. Wetting kinetics and LHR values of coal and kaolinite before and after absorbing PAM A401 (in 12 mg·dm^{-3}, at 20 °C)

Samples	c (10^{-6} cm^5)	*n*-Hexane		Deionized water		LHR
		k (g^2·s^{-1})	Regression Coefficient	k (g^2·s^{-1})	Regression Coefficient	
Coal	2.12E-06	0.0050	0.9998	0.0016	0.9995	9.23
Coal adsorbed PAM A401	1.81E-06	0.0045	0.9997	0.0018	0.9994	7.28
Kaolinite	5.68E-06	0.0101	0.9998	0.0206	0.9996	1.44
Kaolinite adsorbed PAM A401	2.16E-06	0.0076	0.9999	0.0135	0.9999	1.65

Linear stages were obtained from the wetting curves given in Figs. 12 and 13 by removing several of the initial points and the wetting equilibrium points. A linear least-squares fit for all wetting rates gave regression coefficients greater than 0.9994. Table 7 showed that the wetting rate of samples by water was as follows: kaolinite > kaolinite with adsorbed PAM A401 > coal with adsorbed PAM A401 > coal, while the wetting rate by *n*-hexane was as follows: kaolinite > kaolinite with adsorbed PAM A401 > coal > coal with adsorbed PAM A401. The different surface chemistries of the particles led to different wetting curves. The LHR value was calculated by Eq. (11). Greater LHR values were associated with more hydrophobic powder samples and vice versa. Kaolinite (LHR 1.44) was more hydrophilic than the coal sample (LHR 9.23). After the adsorption of PAM A401, the LHR of coal decreased from 9.23 to 7.28,

indicating that the coal became less hydrophobic than before. In contrast, the LHR of kaolinite increased from 1.44 to 1.65. The wettability changes in coal or kaolinite would be deleterious to flotation.

Selective floc flotation test

Both the selective enlargement of the particle size and the wettability changes of coal and kaolinite would affect the fine coal separation. Table 8 showed that the adsorption difference of PAM A401 onto coal or kaolinite strengthens the fine particle flotation. Selective floc flotation of the fine coal was better than the flotation without PAM A401. The combustible recovery yield was increased by 8.21%, while the clean coal ash was 11.67%.

Table 8. Effect of PAM A401 on the selective floc flotation

Dose $(g \cdot Mg^{-1})$	Clean Coal		Reject		Combustible	Calculated Ash of the
PAM A401	Yield (%)	Ash (%)	Yield (%)	Ash (%)	Recovery (%)	Feed (%)
0	55.29	11.55	44.71	57.44	71.99	32.07
2	61.90	11.67	38.10	64.56	80.20	31.82

Summary and conclusions

The adsorption behavior of anionic polyacrylamide PAM A401 onto kaolinite and coal was investigated at the low concentration of 0–16 mg·dm^{-3}. The results indicated that PAM A401 was selectively adsorbed onto ultra-low ash coal rather than kaolinite. Physical adsorption was the predominant mechanism, and the adsorption of PAM A401 at 12 mg· dm^{-3} onto coal was 2.15 times larger than the adsorption on kaolinite. Different adsorptions resulted in wettability changes for coal and kaolinite, but selective enlargement of the coal particle size strengthened the fine coal flotation. After the adsorption of PAM A401, the LHR of coal decreased from 9.23 to 7.28. In contrast, the LHR of kaolinite increased from 1.44 to 1.65. Characteristic parameters of particle size of the d_{10}, d_{50} and d_{90} of coal flocculated by PAM A401 (at 12 mg/dm^3, pH 6.5) were 3.18, 2.76 and 2.59 times of the corresponding levels of these parameters for kaolinite floc, respectively.

Acknowledgments

References

BESRA L., SENGUPTA D. K., ROY S. K., AY P., 2004. *Influence of polymer adsorption and conformation on flocculation and dewatering of kaolin suspension*. Separation and Purification Technology, 37(3), 231-246.

CAULFIELD M. J., QIAO G. G., SOLOMON D. H., 2002. *Some aspects of the properties and degradation of polyacrylamides*. Chemical Reviews, 102(9), 3067-3084.

CHANG Q., WEI B.G., HE Y. D., 2009. *Capillary pressure method for measuring lipophilic hydrophilic ratio of filter media*. Chemical Engineering Journal, 150 (2-3), 323–327.

HOGG R., 1980. *Flocculation problems in the coal industry*. Fine Particles Processing, 2, 990-999.

HORSFALL JNR M., SPIFF A. I., 2005. *Effects of temperature on the sorption of Pb^{2+} and Cd^{2+} from aqueous solution by Caladium bicolor (Wild Cocoyam) biomass*. Electronic Journal of Biotechnology, 8(2), 43-50.

JENKINS P., RALSTON J., 1998. *The adsorption of a polysaccharide at the talc–aqueous solution interface*. Colloids and Surfaces A: Physicochemical and Engineering Aspects, 139(1), 27-40.

KHAN A. A., SINGH, R. P., 1987. *Adsorption thermodynamics of carbofuran on Sn(IV) arsenosilicate in H^+, Na^+ and Ca^{2+} forms*. Colloids and Surfaces, 24(1), 33-42.

MAO J. D., SCHIMMELMANN A., MASTALERZ M., HATCHER P. G., LI Y., 2010, *Structural features of a bituminous coal and their changes during low-temperature oxidation and loss of volatiles investigated by advanced solid-state NMR spectroscopy*. Energy & Fuels, 24(4), 2536-2544.

MILLER J. D., LASKOWSKI J. S., CHANG S. S., 1983. *Dextrin adsorption by oxidized coal*. Colloids and Surfaces, 8(2), 137-151.

NASSER M. S., JAMES A. E., 2006. *The effect of polyacrylamide charge density and molecular weight on the flocculation and sedimentation behaviour of kaolinite suspensions*. Separation and Purification Technology, 52(2), 241-252.

PAROLIS L., GROENMEYER G., HARRIS P., 2005. *Equilibrium adsorption studies of polysaccharides on talc: The effects of molecular weight and charge and the influence of metal cations*. Minerals and Metallurgical Processing, 22(1), 12-16.

PARIA S., KHILAR K. C., 2004. *A review on experimental studies of surfactant adsorption at the hydrophilic solid–water interface*. Advances in Colloid and Interface Science, 110(3), 75-95.

PEARSE M. J., 2005. *An overview of the use of chemical reagents in mineral processing*. Minerals Engineering, 18(2), 139-149.

SABAH E., ERKAN Z. E. 2006. *Interaction mechanism of flocculants with coal waste slurry*. Fuel, 85(3), 350-359.

SCOGGINS M. W., MILLER J. W., 1979. *Determination of water-soluble polymers containing primary amide groups using the starch-triiodide method*. Society of Petroleum Engineers Journal, 19(03), 151-154.

SEDEVA I. G., FORNASIERO D., RALSTON J., BEATTIE D. A., 2010. *Reduction of surface hydrophobicity using a stimulus-responsive polysaccharide*. Langmuir, 26(20), 15865-15874.

SPENCER L., BROOKES G. F., 1987. *Polyacrylamides and the selective flocculation of coal/shale mixtures*. Coal Preparation, 4(1-2), 133-159.

TAYLOR M. L., MORRIS G. E., SELF P. G., SMART R. S. C., 2002. *Kinetics of adsorption of high molecular weight anionic polyacrylamide onto kaolinite: the flocculation process*. Journal of Colloid and Interface Science, 250(1), 28-36.

VAN OLPHEN H., HSU P. H. 1978. *An Introduction to Clay Colloid Chemistry*. Soil Science, 126(1), 59.

WASHBURN E. W. 1921. *The dynamics of capillary flow*. Physical Review, 17(3), 273-283.

XU Z., LIU J., CHOUNG J. W., ZHOU Z., 2003. *Electrokinetic study of clay interactions with coal in flotation*. International Journal of Mineral Processing, 68(1), 183-196.

ZHANG Z. J., LIU J. T., FENG L., WANG Y. T., 2012. *A method of laser particle size analysis for evaluating coagulation of coal slime*. Journal of China University of Mining & Technology, 41(4), 624-628.

ZHU H. Y., JIANG R., XIAO L., ZENG G. M., 2010. *Preparation, characterization, adsorption kinetics and thermodynamics of novel magnetic chitosan enwrapping nanosized γ-Fe2O3 and multi-walled carbon nanotubes with enhanced adsorption properties for methyl orange*. Bioresource Technology, 101(14), 5063-5069.

ZOU W., CAO Y., LIU J., LI W., LIU C., 2013. *Wetting process and surface free energy components of two fine liberated middling bituminous coals and their flotation behaviors*. Powder Technology, 246, 669-676.